

Plasma double layer system leading to chaos, intermittency and flicker noise

A.J. TURSKI and B. ATAMANIUK (WARSZAWA)

ELECTROSTATIC DOUBLE LAYERS appear in plasma and semiconductor systems with flow of electric current. The systems display bifurcations, chaos, intermittency and power-law of spectral power density that is $1/f$ -noise also called flicker noise. Fractal analysis of experimental data recorded in time (time-series analysis) indicates that the plasma dynamic systems are of low dimension. Colored and fractal noise influence on measured data may disqualify that conclusion. A piecewise linear dynamical system is considered to clarify this problem. Bifurcation tree, intermittent chaos and $1/f$ -noise are revealed by the dynamic system.

1. Introduction

THE STUDY OF PLASMA systems may be performed by analyzing experimental data recorded as a series of measurements in time of pertinent and easily accessible state variables of the system, e.g. electric current, voltage, densities and velocities. In most cases, such variables describe a global or averaged properties of the system. Although there already exists a vast literature describing experimental results concerning bifurcation, intermittency and chaos in plasma discharge and turbulent systems, a complete and coherent discussion and theory derived from plasma equations are still lacking. Plasma discharges produced by electric current flow and revealing self-oscillations (Hopf bifurcation), saddle-node and period-doubling bifurcations, intermittency and chaos are of our interest. We assume that the cause of the occurring phenomena is charge separation leading to double layers (DL), which are localized in space. The wave length of the wave phenomena is much greater than the physical size of the system and we can consider DL as a lumped element. The assumption allow us to construct a simplified model. It is based on piecewise linear voltage-charge characteristic of a capacitor simulating DL. The model can be realized in the form of nonlinear electrical circuit and the measured variables are to be compared with those analytically computed. By virtue of the circuit equation analysis [1], Poincaré map is derived. Calculation of bifurcation trees and strange attractors for different parameter sets are displayed and intermittency, saddle-node and period-doubling bifurcations are revealed.

Plasma experimental data recorded as a series of measurements in time are analyzed by use of fractal dimension and the average dimension, most often correlation dimension, is low and that implies the low-dimensional dynamical system [2, 3]. This conclusion was very recently criticized for the two reasons. One stems from the fact that the apparent correlation dimension may result from the class of

stochastic noises with a power-law of spectral power density, $f^{-\alpha}$, the so-called colored noise, which leads to a low finite value for the correlation dimension, see [4]. The second reason is related to intermittency which leads to the same power-law spectra and low fractal dimension. The low correlation dimension of such noise means that the trajectories in the state space exhibit fractal behaviour along the trajectories, while the fractality of a strange attractor associated with a chaotic system is perpendicular to the motion such that each trajectory returns at time close to the starting points. The methods which have been used in the studies of the correlation dimension [3, 4] do not distinguish between these two kinds of fractalities. The situation around this topic has remained unclear and we offer some nonlinear circuit analogue models, which show promising results. We introduce two notions – one is a colored stochastic noise and its power-law spectra for low frequencies, and the other one is intermittent chaos leading to $f^{-\alpha}$ noise. It deserves notice that the $f^{-\alpha}$ noises are ubiquitous phenomena concerning elements of electronics, acoustics, mechanics, traffics, etc., see [5, 6, 7]. Consideration of dynamical system with piecewise linear nonlinearity may contribute to understanding of the problem.

2. Colored noise

Colored stochastic noise $\eta(t)$ is based on an extension of the space of variables so that $\eta(t)$ itself becomes a variable driven by white noise $\zeta(t)$. In particular, if $\eta(t)$ is exponentially correlated Gaussian noise then one can write the set of stochastic differential equations

$$(2.1) \quad \dot{x}(t) = G(x) + g(x)\eta(t),$$

$$(2.2) \quad \dot{\eta}(t) = -\frac{1}{\tau_c}\eta(t) + \zeta(t),$$

where $G(x)$ is the deterministic “force” and $\zeta(t)$ is Gaussian white noise with correlation function

$$(2.3) \quad \langle \zeta(t)\zeta(\tau) \rangle = 2D \delta(t - \tau).$$

Then it can be easily seen that (2.2) leads to the exponential correlation function

$$(2.4) \quad \langle \eta(t)\eta(\tau) \rangle = \frac{D}{\tau_c} e^{-\frac{|t-\tau|}{\tau_c}}.$$

The probability density $P(x, \eta; (t/x_0), \eta_0)$ obeys a Fokker–Planck equation. Bicolored stochastic noise assumes two additional variables $\eta_1(t)$ and $\eta_2(t)$ with constants τ_{c1} and τ_{c2} , see Eq.(2.2), driven by white noises with D_1 and D_2 , respectively.

We note that colored noise had a low correlation dimension as determined from the Grassberger – Procaccia (GP) algorithm [4]. The stochastic process generated by one or two colors can be expressed as discrete Fourier series [4]

$$(2.5) \quad X(i) = \sum_{k=1}^{N/2} C_k \cos(2\pi i k/N - \phi_k),$$

where ϕ_k are random phases in the range $[0, 2\pi]$ for each wave number k , $f = k/N$ is a frequency, and the coefficients C_k are related to the power spectrum $P(k) = Q k^{-\alpha}$, that is

$$(2.6) \quad C_k = \left[P(k) \frac{2\pi}{N} \right]^{1/2}$$

for bicolored noise, we have two powers α_1, α_2 , and α_1 is valid for the range $k < k_c$ and α_2 is valid for $k > k_c$. Critical value k_c is such that it relates to a frequency at which there is a break in the power spectrum of the measured variable. The condition of continuity is fulfilled if $Q_1 k^{-\alpha_1} = Q_2 k^{-\alpha_2}$.

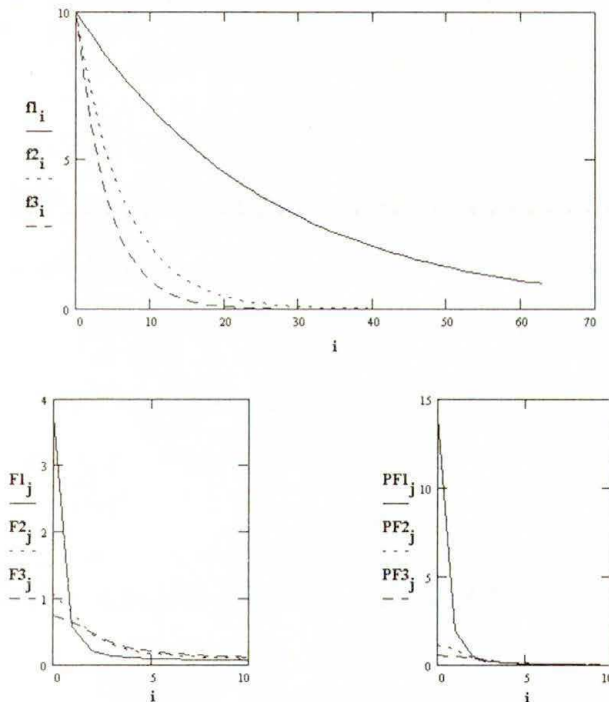


FIG. 1. Exponential correlation functions – $f1_i, f2_i, f3_i$ versus i , related Fourier transforms $F1_j, F2_j, F3_j$ and power Fourier transforms $PF1_j, PF2_j, PF3_j$ versus j .

Computer calculated and plotted Fig. 1 refers to the correlation functions (2.4) and exhibits $f_{l,i} = A \exp(-k_l t_i)$, where $l = 1, 2, 3; k_1 = 0.25, k_2 = 1, k_3 = 1.5$

and $t_i = 0 \div 63$. Also Fourier transforms $F_{1,j} = FFT(f_1)$, $F_{2,j}$, $F_{3,j}$ are shown as well as power spectra $PF_{1,j} = (|F_{1,j}|)^2$, $PF_{2,j}$, and $PF_{3,j}$ are depicted.

The Fourier transform

$$(2.7) \quad F_{l,j} = \frac{A_l}{\pi} \frac{1}{\omega_j^2 + k_l^2}, \quad l = 1, 2, 3$$

is the well known Lorentzian spectral density revealing flicker noise. This approach is to be used in cases of more complex correlation functions.

3. Intermittency and flicker noises

The phenomena of flicker noise have long posed some enigmatic questions. First and foremost is the question of how is it possible that in systems of minute physical size there occur processes on the time scale so long as to allow for divergences in their spectra? The appearance of broadband spectra and, at the same time, the rising of the low-frequency end have long been associated with the onset of chaotic behaviour. Chaotic signals as well as stochastic ones are assumed to have stationary statistic and the correlation function

$$(3.1) \quad \langle x(t) x(\tau) \rangle \equiv C_x(\tau).$$

Since noise waves have infinite energy but finite power, we must define a power spectral density.

The autocorrelation function for a noise wave $x(t)$ is defined as the time average

$$(3.2) \quad C_x(\tau) \equiv \lim_{T \rightarrow \infty} \frac{1}{2T} \int_{-T}^T x(t + \tau) x(t) dt$$

and then

$$C_x(\tau) = C_x(-\tau).$$

The spectral density of the noise wave $x(t)$ is defined as the Fourier transform

$$(3.3) \quad S_x(f) = \int_{-\infty}^{\infty} C(\tau) e^{-2\pi i \tau f} d\tau,$$

where $S_x(f)$ must be real and positive and if $x(t)$ is real, we have

$$S_x(f) = S_x(-f).$$

Bifurcation and chaotic features of dynamical systems of finite number of freedom-degrees are investigated by use of Poincaré maps, which are discrete processes. In case of one-dimensional map

$$(3.4) \quad x_{n+1} = g(x_n),$$

the discrete autocorrelation function $C_x(m)$ of x_n is

$$(3.5) \quad C_x(m) = \lim_{N \rightarrow \infty} \frac{1}{2N + 1} \sum_{n=-N}^N x_{n+m} x_n,$$

and spectral density

$$(3.6) \quad S_x(f) = \sum_{m=-\infty}^{\infty} C_x(m) e^{-2\pi mif}.$$

By virtue of symmetry, we have

$$(3.7) \quad S_f = \sum_{m=0}^{\infty} C(m) \cos(2\pi mf),$$

where

$$(3.8) \quad C_x(m) = \lim_{N \rightarrow \infty} \frac{1}{N} \sum_{n=0}^N x_{n+m} x_n.$$

Let us consider a logistic map

$$(3.9) \quad x_{n+1} = Rx_n(1 + x_n) \equiv g(x_n)$$

where $0 < R < 4$.

Just below period 3, there is a saddle-node bifurcation for $R_c = 1 + (8)^{1/2}$ and then at $R = R_c - \varepsilon$, an intermittent signal appears. For any $\varepsilon > 0$, correlation functions $C_x(m)$ decay exponentially with a decay time $\tau \sim \varepsilon^{-1/2}$, see [5]. By plotting the power spectrum of the third iterate $g^3(x)$ we can thus get an apparent $1/f^2$ divergence, with a cut-off that can again be pushed down to arbitrarily small frequencies by lowering ε . There are three types of intermittencies. The first one is connected with transition from saddle-node bifurcation to chaos, second with Hopf bifurcation and the third one with period doubling bifurcation. Figure 2 demonstrates the computed results of the intermittent signal x_n versus n for $R = 3.74474 < R_c$, its correlation function

$$(3.10) \quad C_s = \frac{1}{N + 2 - s} \left(\sum_{k=0}^{N+1-s} x_{k+s} x_s \right)$$

and Fourier transform $KC_s := FFT(C_s)$ as well as power spectral density, that is $PKC_s := (|KC_s|)^2$. Spectral densities reveal $1/f$ divergence in vicinity of $f = 0$, ($s = 0$). This approach is to be used in cases of more complex Poincaré maps.

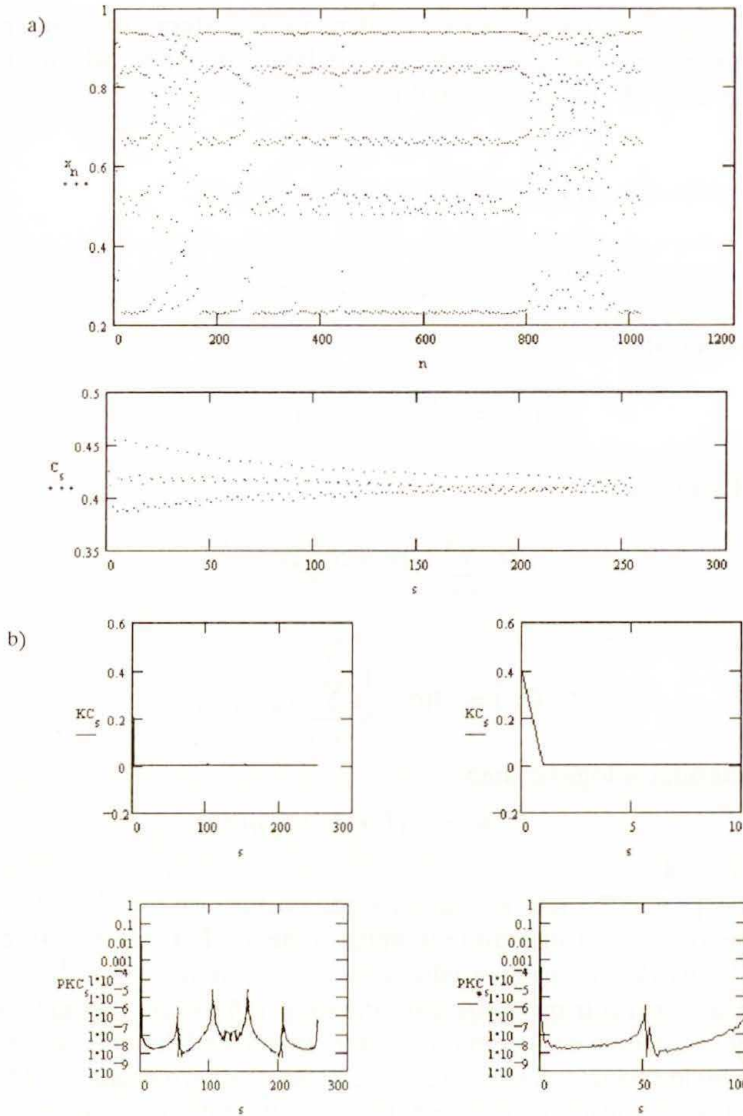


FIG. 2. a) Intermittent signal x_n versus n for logistic map $x_{n+1} = Rx_n(1 - x_n)$ where $R = 3.74474$ and its correlation function C_s . b) Fourier transform KC_s , and PKC_s versus s . The right-hand side drawings of KC_s and PKC_s are enlarged in vicinity of $s = 0$ and demonstrate $1/f$ - noise behaviour.

4. Charge separation and double layer simulations

Charge separation in plasmas takes place due to electric current flow. Formation of DL starts when electron and ion convection velocities of the flow satisfy Bohm conditions, e.g. see Galeev and Sagdeev, Ch. 1 in the monograph [8]. The

negative anomalous resistivity of plasma discharges leads to self-oscillation [9] and then nonlinear voltage-charge characteristic is responsible for bifurcation, intermittency and chaos. The characteristic is similar, if not identical, to that of junction capacitance of semiconductor diode, which is based on charge separation. Self-oscillations of plasma discharges are revealed by use of electrical circuit with nonlinear resistance, e.g. see [10]. The problem is classical in plasma discharges. The next step is a simulation of plasma discharge system by a driven R–L–Diode circuit, see [1, 9]. The circuit ordinary differential equations are reduced to the following 2-D Poincaré map [1, 9]:

$$(4.1) \quad \begin{aligned} x_{n+1} &= y_n - 1 + \begin{cases} a_1 x_n & \text{for } x_n \geq 0, \\ -a_2 x_n & \text{for } x_n < 0, \end{cases} \\ y_{n+1} &= b x_n, \end{aligned}$$

where x_n and y_n are responsible for charge and current in the circuit, and

$$(4.2) \quad \begin{aligned} a_1 &= e^{\lambda_1} + e^{\lambda_2}, \\ b &= -e^{\lambda_1 + \lambda_2} = -e^{-R/2Lf}, \\ \lambda_{1,2} &= -\frac{R}{2Lf} \pm \frac{1}{2f} \left[\left(\frac{R}{L} \right)^2 - \frac{4}{LC_{1,2}} \right]^{1/2}. \end{aligned}$$

R, L, C_1, C_2 are circuit elements and f is the frequency of the driving voltage. Characteristic values $\lambda_{1,2}$ are real or complex conjugate, hence a_1 and b are always real positive and real negative numbers, respectively. A piecewise linear characteristic (C_1, C_2) is a satisfactory substitute for the nonlinear voltage-charge characteristic, see [1, 9]. The coefficient a_2 depends on amplitude and frequency of the driving voltage and can be numerically determined. The graphs of a_2 versus driving voltage for a given number of frequencies f are given in [1]. We note, that the following equation

$$(4.3) \quad \frac{d^2u}{dt^2} + k \frac{du}{dt} + f(u) + E_0 = E(t),$$

where

$$f(u) = \begin{cases} \alpha u & \text{for } u \geq 0, \\ \beta u & \text{for } u < 0 \end{cases}$$

is a piecewise linear function and

$$E(t) = E^0 \sin(\omega t) \simeq \text{sgn}(\sin(\omega t)),$$

possesses the Poincaré map given by Eq.(4.1).

From extensive laboratory measurements and digital computer simulations, S. TANAKA *et al.* [1], have found that in order to reproduce the same qualitative

behaviour of the dynamical system, a piecewise linear voltage-charge characteristic is satisfactory. Furthermore, it was observed that the sinusoidal voltage source can be replaced by square wave voltage of the source period $T = 1/f$ without altering the bifurcation structures. Therefore, we analyze Eq.(4.1) as a structure representing dynamics of the system with a nonlinear element responsible for charge separation. We believe, that intermittent chaos and flicker noise have not yet been revealed for the system. We exhibit our numerical calculation results. Figure 3 shows the “bifurcation tree” that is $x_{l,m}$ versus a_2 where $l = 650, 651, \dots, 750$ represents the iteration number, see Eq.(4.1) where $n = l$, whereas m is responsible for $a_2(m)$, which changes from 0 to 10 as m changes from 0 to M , e.g. $M = 200$. The second variable $y_{l,m}$ is similar since $y_{l+1,m} = bx_{l,m}$. It reflects the physical situation that each point in this bifurcation tree diagram represents a 1-D Poincaré section of electric current trajectory taken at each fundamental period $T = 1/f$ of the sinusoidal voltage source. Iteration results for $l = 0, 1, 2, \dots, 649$ are not depicted here. They concern mainly transition points to periodic and chaotic states. The following striking features are seen in this diagram.

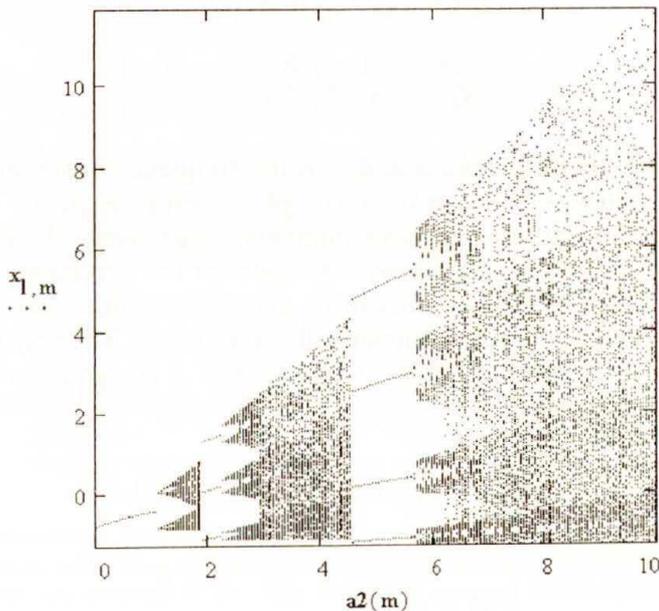


FIG. 3. Bifurcation tree of Eq.(4.1), $l = 650, \dots, 750$, l is iteration number $n \leftrightarrow l$ and m is responsible for $a_2(m)$ changes along horizontal axis.

(i) A succession of large periodic windows whose periods increase exactly by one as we move from one window to the next at its right side (saddle-node bifurcation). On the left side of each chaotic band we observe transition to chaos via period-doubling bifurcation.

(ii) Going along trajectories we can expect a 1st-type intermittency at the right-hand side of boundary of each band of chaos and a 3rd-type one at the left side of the boundary of chaotic bands.

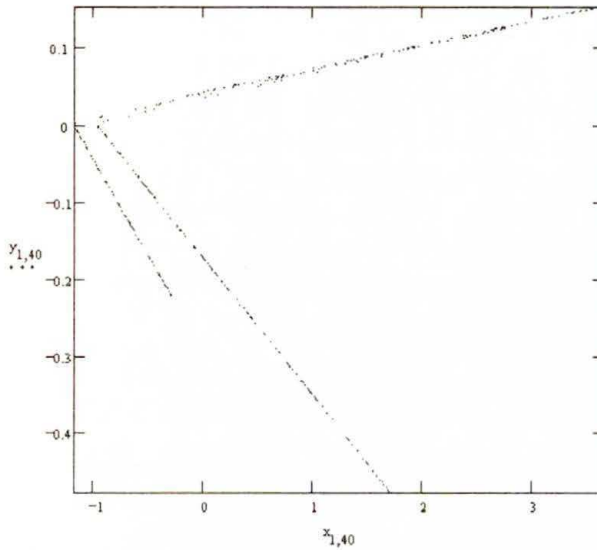


FIG. 4. Strange attractor for $a_2 = 4$.

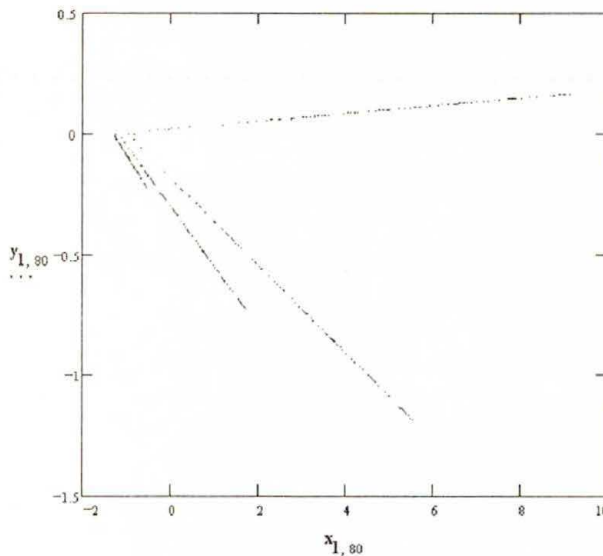


FIG. 5. Strange attractor for $a_2 = 8$.

Figures 4 and 5 show a 2-D Poincaré sections taken for $a_2 = 4$ and $a_2 = 8$, that is the second and third chaotic bands, see Fig. 3. They are strange attractors associated with a chaotic motion perpendicular to the trajectories. The attractors

are composed of a number of branches and the number increases as we move from left to the right bands.

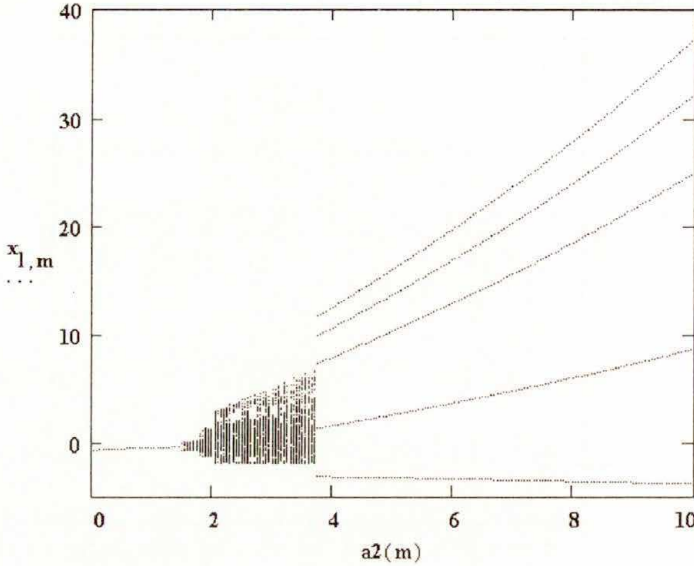


FIG. 6. Bifurcation tree for Eq. (4.1), $x_{l,m}$ versus $a_2(m) \Rightarrow m$, where l is iteration number and $a_1 = 1.13$, $b = -0.5$.

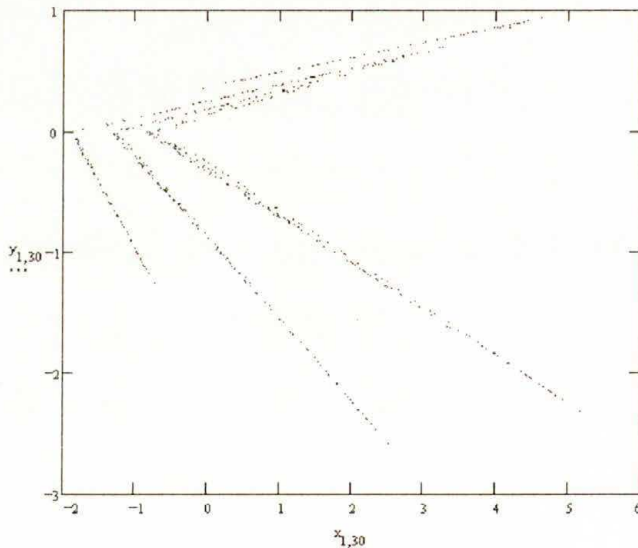


FIG. 7. Strange attractor for $a_2 = 3$.

Figures 6, 7 and 8 show the bifurcation tree and strange attractors for selected parameters $a_1 = 1.13$ and $b = -0.5$. There is only one chaotic band and two large periodic windows. The strange attractors are composed of 5 branches for $a_2 = 3$

and 3.5. The number of periods jumps from 1 to 5 as we move from left to the right-hand periodic windows. One can expect $1/f$ fluctuations along trajectories due to the 1-st and 3-rd- type of intermittency.

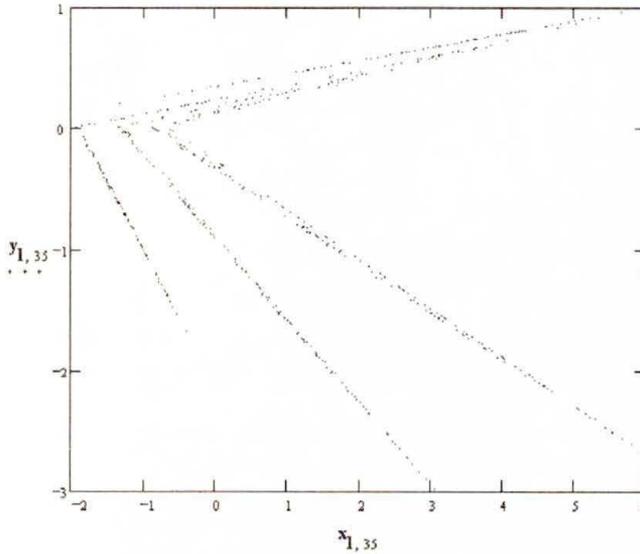


FIG. 8. Strange attractor for $a_2 = 3.5$.

Figure 9 exhibits computed Lyapunov exponents λ_x determining variation of x_n versus a_2 for the bifurcation tree depicted above. We note that the calculated negative values of λ_x and stable periodic windows of the bifurcation tree as well as positive values of λ_x and chaotic band are related, respectively.

To demonstrate intermittency of our system given by Eq. (4.1) we determined a number of values of a_2 for which intermittent chaos occurs. We may expect such values of a_2 at the transition of periodic windows and chaotic bands. It is worth noting that, in some cases, very high precision of calculation of a_2 is necessary.

Figure 10 shows intermittent state variable (signal) x_n versus n , strange attractor y_n versus x_n , power spectrum PX_n that is a fast Fourier transform (FFT) of x_n^2 , correlation function C_s computed according to Eq. (3.10) and its power spectrum density for a selected value $a_2 = 1.94610199282$. This figure shows intermittency of saddle-node type, which is located at the boundary of the first chaos band and 3-period window, see Fig. 3. The intermittent signal consists of chaotic part and inclusions of 2, 3 and 4-periodic parts. Also, the strange attractor reveals periodic parts in the form of isolated points. Power spectrum density $-PX_n$ displays $1/f$ fluctuations (flicker noise) in the vicinity of $n = 0$. The correlation function diagram and the power spectrum of the function confirm this property.

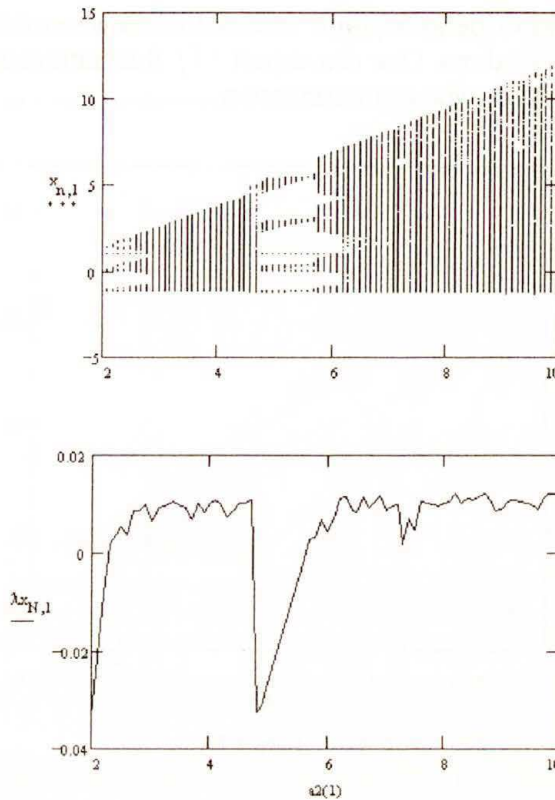


FIG. 9. Lyapunov exponent λ_x versus a_2 in relation to bifurcation tree of Eq. (4.1) $a_1 = 0.7$, $b = -0.13$, and $a_2 = 0 \div 10$.

Figures 11 and 12 show two intermittently chaotic regimes. They concern transition from the chaotic band to the 4-periodic window (Fig. 3). For a given value of a_2 , see Fig. 11, we have predominantly chaotic x_n but if we add only 10^{-14} to a_2 then x_n changes drastically (4-periodicity prevails). The shape of strange attractors is nearly the same but that one responsible for the more chaotic case seems to be more “dense”. Also here, the power spectrum has no sharp peaks, in contrast to the less chaotic case. Correlation functions are distinctly different. One is similar to the purely chaotic correlation and the other one to the periodic case. Flicker noise components are more significant for the case of less chaotic variable.

The last figure, Fig. 13, shows the state variable x_n versus n for the bifurcation tree presented in Fig. 6. We found the value of $a_2 = 3.7241$, which is characteristic for a transition from chaotic band to 5-periodic window. The selected value of a_2 is such that nearly a half of the variable x_n is chaotic and a half is 5-periodic. Power spectrum correlation function and flicker noise contributions are characteristic for intermittency.

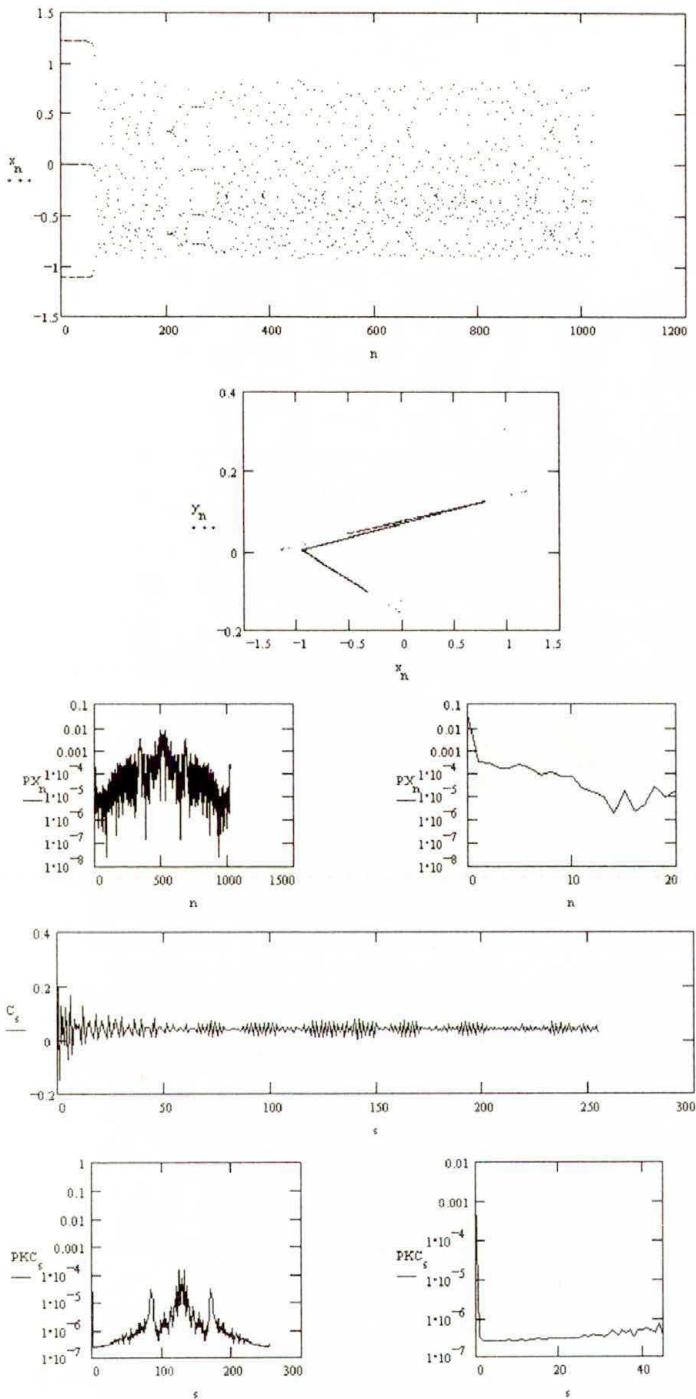


FIG. 10. Intermittent state variable x_n versus n (here time), strange attractor y_n versus x_n , power spectrum $PX_n = FFT(x_n^2)$ versus n (here frequency), the correlation function C_s versus s (here time) computed according to Eq. (3.10) and its power spectrum $PKC_s = FFT(C_s^2)$ versus s (here frequency). Parameter of Eq. (4.1); $a_1 = 0.7$, $b = -0.13$ and $a_1 = 1.94610199282$.

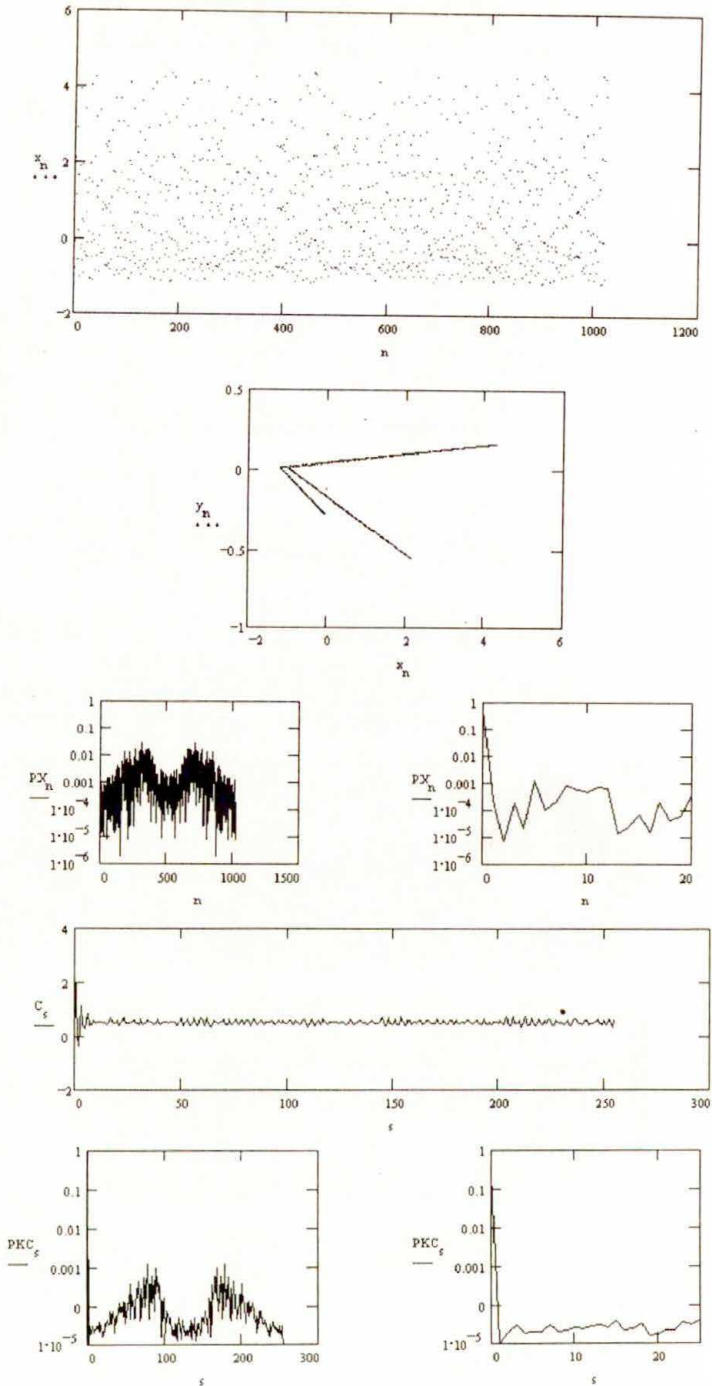


FIG. 11. Intermittent state variable x_n versus n (here time), strange attractor y_n versus x_n , power spectrum $PX_n = FFT(x_n^2)$ versus n (here frequency), the correlation function C_s versus s (here time) computed according to Eq. (3.10) and its power spectrum $PKC_s = FFT(C_s^2)$ versus s (here frequency). Parameter of Eq. (4.1); $a_1 = 0.7$, $b = -0.13$ and $a_2 = 4.57988001000011$.

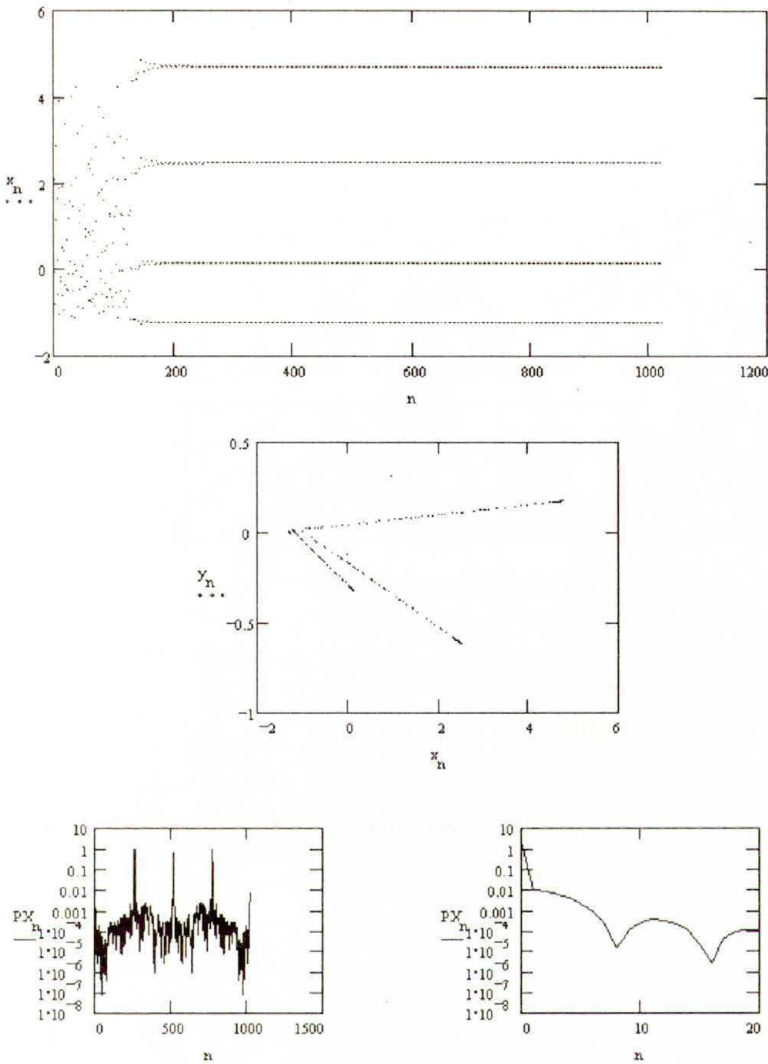


FIG. 12. Intermittent state variable x_n versus n (here time), strange attractor y_n versus x_n , power spectrum $PX_n = FFT(x_n^2)$ versus n (here frequency). Parameter of Eq. (4.1); $a_1 = 0.7$, $b = -0.13$ and $a_2 = 4.57988001000012$.

The intermittent signals presented here were selected from a great number of computed examples of chaotic regimes. We note that the state variable y_n can be easily obtained in virtue of the following relation: $y_{n+1} = bx_n$, see Eq. (4.1). We see that the chaotic bands are self-similar and therefore, intermittent variables x_n can be found inside of each chaotic band. For instance, the central chaotic band of Fig. 3 is composed of three self-similar sections, which appear as we divide the band by two horizontal lines and each section is similar to the entity. The same property shows all chaotic bands of Fig. 3.

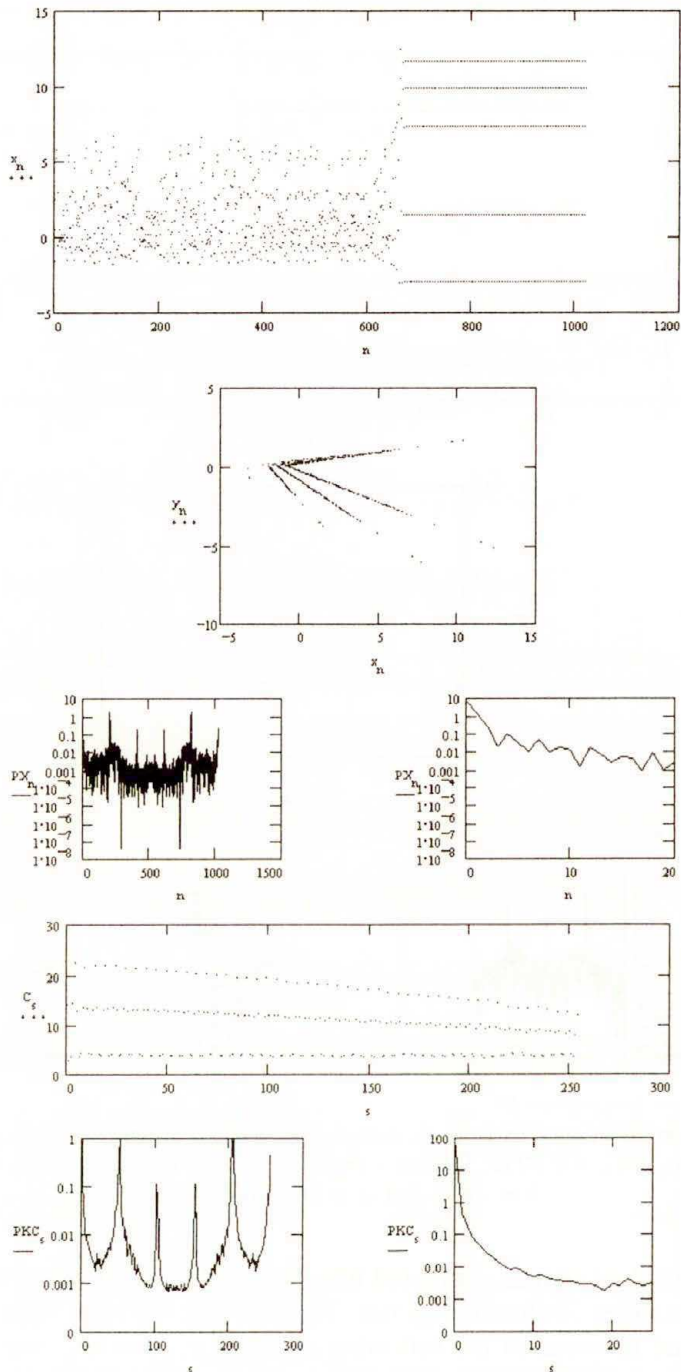


FIG. 13. Intermittent state variable x_n versus n (here time), strange attractor y_n versus x_n , power spectrum $PX_n = FFT(x_n^2)$ versus n (here frequency), the correlation function C_s versus s (here time) computed according to Eq. (3.10) and its power spectrum $PKC_s = FFT(C_s^2)$ versus s (here frequency). Parameter of Eq. (4.1); $a_1 = 1.13$, $b = -0.5$ and $a_2 = 3.7241$.

5. Conclusions

The dynamical system considered here is advantageous as it may be easily measured and computed. There are three parameters a_1 , b and a_2 which allow for applications and simulations of different dynamical processes. Three fundamental features deserve attention. The assumed piecewise linear approximations of nonlinear characteristics allow to expose the most complex properties of nonlinear systems, e.g. important types of bifurcations, self-similarity, chaos, intermittency, fractality and flicker noise. A number of papers are devoted to the theory of piecewise linear maps, we refer to the following [5, 11, 12] and [13].

The next features concern flicker noise or $1/f$ fluctuations of intermittently chaotic variables. In principle, we are not able to distinguish colored noise, coming from outside to the system, from the intermittent signal of the system, which generates the noise. In the case of colored noise, however, the trajectory produces a fractal curve that wanders erratically; the correlation dimension is a measure of the fractal dimension of this curve and is unrelated to the existence of an attractor. In addition, the correlation dimension is related to the power law spectral index $\alpha(f^{-\alpha})$ by $D_{cr} = 2/(\alpha - 1)$, see [4]. Fractal dimension of strange attractors is the last feature of our comments. Varying the parameter a_2 we may select intermittently chaotic variable of higher or lower contents of chaos. In this way, we may change fractal dimensions of an attractor as well as the power law spectral index α . According to our computer calculations, lowering content of chaos in intermittent signal causes higher content of $f^{-\alpha}$ fluctuations but lowers fractal dimension of strange attractors. This conclusion concerns only the ranges of parameters a_1 , b and a_2 considered here.

Acknowledgments

The paper was partly supported by the State Committee for Scientific Research (KBN) through the grant No. 2P03C01210.

References

1. S. TANAKA, T. MATSUMOTO and CHUA, *Bifurcation scenario in a driven R-L-diode circuit*, *Physica*, **28D**, 317–344, 1987.
2. D. WEIXING, H. WEI, W. XIAODONG and C.X. YU, *Quasiperiodic transition to chaos in a plasma*, *Phys. Rev. Lett.*, **70**, 170–173, 1993.
3. T. KLINGER and A. PIEL, *Investigations of attractors arising from the interaction of drift waves and potential relaxation instabilities*, *Phys. Fluids*, **B4**, 12, 3990, 1992.
4. A.S. OSBORN and A. PROVANZALE, *Finite correlation dimension for stochastic system with power-law spectra*, *Physica*, **D35**, 357, 1989.
5. H.G. SCHUSTER, *Deterministic chaos. An introduction*, Second revised Ed., VCH Verlagsgesellschaft, Weinheim, Germany 1988.
6. E. INFELD and G. ROWLANDS, *Nonlinear waves, solitons and chaos*, Cambridge University Press, Cambridge 1992.

7. J. HIRSH, B. HUBERMAN and D. SCALPINO, *Theory of intermittency*, Phys. Rev., A **25**, 1, 519–532, 1982.
8. R.Z. SAGDEEV and M.N. ROZENBLUTH, *Foundation of plasma physics* [in Russian], Vol. 2, Supple., Energo Atomizdat, Moskva 1984.
9. A.J. TURSKI, *Modelling of aurora double layers leading to oscillations and chaos*, Part 1 [in Polish], IFTR Report, 38, 1989; and Part 2, IFTR Reports, 20, 1990.
10. N. MINORSKY, *Nonlinear oscillations*, D. Van Nostrand Co., Toronto-New York-London 1962.
11. T. TÉL, *Invariant curves, attractors, and phase diagram of piecewise linear map with chaos*, J. Stat. Phys., **33**, 1, 195–221, 1983.
12. T. TÉL, *Fractal dimension of the strange attractor in piecewise linear two-dimensional map*, Phys. Lett., **971**, 6, 219–223, 1983.
13. V. MAISTRENKO and I. SUSHKO, *Period adding phenomenon in piecewise linear endomorphism arising from electronic systems*, Proc. of the Workshop NDES–94, Kraków, Poland, 39–44, 1994.

POLISH ACADEMY OF SCIENCES
INSTITUTE OF FUNDAMENTAL TECHNOLOGICAL RESEARCH

e-mail: aturski@ippt.gov.pl

e-mail: bataman@ippt.gov.pl

Received August 28, 1996.